

EXPERIMENTAL POLYMICROBIAL PERITONITIS–ASSOCIATED TRANSCRIPTIONAL REGULATION OF MURINE ENDOGENOUS RETROVIRUSES

Kiho Cho,* Sophia Chiu,* Young-Kwan Lee,* David Greenhalgh,*
and Jean Nemzek†

*Burn Research, Shriners Hospitals for Children Northern California, and Department of Surgery, University of California, Davis, Sacramento, California; and †Unit for Laboratory Animal Medicine and Department of Pathology, University of Michigan, Ann Arbor, Michigan

Received 16 Jun 2008; first review completed 1 Jul 2008; accepted in final form 19 Nov 2008

ABSTRACT—Despite advancements in understanding the pathophysiology of sepsis, clinical outcomes are variable, and the mortality rate remains high among patients. We investigated whether expression of murine endogenous retroviruses (MuERVs), constituting ~10% of the mouse genome, is differentially regulated in response to sepsis-elicited stress signals. ICR mice were subjected to cecal ligation and puncture, and MuERV expression was examined. There was evident regulation (induced or repressed) of MuERV expression in the liver and lung after cecal ligation and puncture. In particular, expression of several variant transcripts was increased, primarily in the liver, at 12 and/or 48 h: nine splicing variants and one 5.06-kb nonspliced transcript. Four novel splicing signals were also identified. Six variant transcripts were presumed to be splicing products of the 5.06-kb transcript, whereas the other three were envelope variants transcribed from at least five MuERV loci. These findings demonstrate that expression of certain MuERVs, including their envelope subgenomic transcripts, are altered during the course of sepsis pathogenesis.

KEYWORDS—Endogenous retrovirus, transcription, splicing variant, polymicrobial sepsis, cecal ligation and puncture

INTRODUCTION

The term sepsis refers to a complex, systemic immune response to infection that can produce serious consequences including multiple organ failure and death. In the United States alone, sepsis is diagnosed in more than 750,000 patients each year with a mortality rate of 29% (1). With the exception of antibiotics introduced in the mid-1900s, there have been few major advancements in the treatment of sepsis. Activated protein C and goal-directed fluid therapy have demonstrated some efficacy; however, these treatments resulted in only modest improvements (2, 3). Consequently, the incidence of sepsis increases each year (1). The increasing incidence is largely due to the complex and heterogeneous nature of host immune responses to sepsis.

Sepsis is a syndrome primarily characterized by both proinflammatory and immunosuppressive host responses to infection. Understanding the complexity of the host response during sepsis will eventually help identify therapeutic targets. It seems that host responses to a specific infection may vary among patients, and appreciation of these differential host responses will be a crucial factor that determines outcomes of the sepsis treatment. These host responses are influenced by a

number of parameters such as age, sex, and environment (4–6). It is likely that genetic profile has a significant role in directing the immune responses to an inflammatory insult stemming from infection (5, 7). In a murine model of sepsis, the mouse strain significantly influenced the immune responses and mortality (7). In clinical studies, several genetic polymorphisms that modulate sepsis severity have been identified in patients (8–10). Hence, it has been suggested that the treatment of sepsis must be individualized to obtain optimal results. This tailored approach for individual patients would be facilitated by a comprehensive understanding of the genetic determinants/elements contributing to the differential host responses to infection.

The genomes of living organisms are rather dynamic structures that constantly interact with the surrounding environments (intracellular as well as extracellular). The genomic variability within human populations is primarily determined by a combination of three different components; sequence polymorphism, epigenetics, and retrotransposition (11–13). First, polymorphisms in genome sequences, including single-nucleotide polymorphism, deletion, and/or insertion, may alter the transcriptional activity and/or function of affected genes. Second, differences in epigenetic modifications, such as genomic DNA methylation and histone acetylation, among individuals affect genome-wide gene expression. Third, transposable elements, including endogenous retroviruses (ERVs), constitute ~45% of the human genome, and it is likely that stress signals (e.g., infection, injury, psychological stress) from the environment may facilitate transposition of these elements into different parts of the genome (14).

Endogenous retroviruses, which are remnants of ancient retroviral infections into the germ line, consist of ~8% of the human genome and ~10% of the mouse genome and are

Address reprint requests to Kiho Cho, PhD, Burn Research, Shriners Hospitals for Children, and Department of Surgery, University of California, Davis, 2425 Stockton Blvd, Sacramento, CA 95817. E-mail: kcho@ucdavis.edu.

This study was supported by grants from Shriners of North America (no. 8680) (to K.C.) and NIGMS (R01GM071360 [to K.C.], GM5486 [to J.N.], and GM067189 [to J.N.]).

Supplemental digital content is available for this article. Direct URL citation appears in the printed text and is provided in the HTML and PDF versions of this article on the journal's website (www.shockjournal.com).

DOI: 10.1097/SHK.0b013e31819721ae

Copyright © 2009 by the Shock Society

transmitted to the offspring in a Mendelian order (15, 16). Each individual's genome has a pool of ERVs inherited from both maternal and paternal genomes. Endogenous retroviruses were often described as "junk DNAs," meaning that they were biologically inactive DNA elements because they were presumed to be incapable of encoding retroviral polypeptides necessary for replication. However, the findings from recent studies implicate ERVs as participants in an array of disease processes, such as autoimmune diseases (e.g., multiple sclerosis, insulin-dependent type 1 diabetes mellitus), cancer, schizophrenia, and injury response (17–23). In particular, ERVs' involvement in autoimmune inflammatory diseases is exemplified by the proinflammatory properties of HERV (human ERV)-W envelope protein, called syncytin, which is reported to be directly responsible for demyelination of oligodendrocytes (17, 18).

In this study, we examine whether expressions of ERVs are altered in response to sepsis-elicited stress signals before a potential investigation into their roles in the confounding etiopathology of sepsis.

MATERIALS AND METHODS

Animals

Female ICR mice (Harlan, Indianapolis, Ind), weighing 20 to 23 g, were used in these experiments. All of the animals were maintained under standard laboratory conditions in the University of Michigan animal housing facility for 5 to 7 days before use. The mice were housed in a temperature-controlled room with a 12-h-light/12-h-dark light cycle. Food and water were provided *ad libitum*. The University Committee on Animal Care and Use approved all of the procedures described in these studies.

Cecal ligation and puncture

The procedure was performed as previously described, and three mice were used in each experimental group (24). The mice were anesthetized with 5% isoflurane and maintained via face mask on 2% to 3% isoflurane in oxygen. The abdomen was prepared for surgery with chlorhexidine solution. A midventral incision (1-cm length) was made in the caudal abdomen. The

cecum was exteriorized, ligated with silk suture, and then punctured twice with a 20-gauge needle. In the ICR mouse, the 20-gauge needle will produce a nonlethal peritonitis. The cecum was then re-placed in the abdomen, and the peritoneal cavity was closed with suture. The skin was closed with tissue glue. Each mouse was given 1 mL of warm lactated Ringer's solution with 5% dextrose s.c. Beginning 2 h after surgery, the animals were given the antibiotic imipenem (25 mg/kg s.c. Primaxin; Merck West Point, Pa) twice daily. The mice were anesthetized with subcutaneous injections of 87 mg/kg ketamine (Ketaset; Fort Dodge Laboratories, Fort Dodge, Iowa) and 13 mg/kg xylazine (Rompun; Bayer Corp, Shawnee Mission, Kans). The mice were then killed by cervical dislocation. Liver and lung samples were removed and snap frozen in liquid nitrogen.

Reverse transcriptase-polymerase chain reaction analysis of murine endogenous retrovirus expression

Protocols for total RNA isolation and cDNA synthesis were described previously (19). Briefly, total RNA was extracted using an RNeasy kit (Qiagen, Valencia, Calif). One hundred nanograms of total RNA was subjected to reverse transcription using Sensiscript reverse transcriptase (Qiagen). Primers, ERV-U1 (5'-CGG GCG ACT CAG TCT ATC GG-3') and ERV-U2 (5'-CAG TAT CAC CAA CTC AAA TC-3'), were used to amplify the 3' U3 regions of noncotropic murine ERVs (MuERVs). The primers for the amplification of full-length/subgenomic transcripts were designed based on a MAIDS (murine acquired immunodeficiency syndrome) virus-related provirus (Mrv) (GenBank no. S80082), and the sequences were as follows: MV1K (5'-CAT TTG GAG GTC CCA CCG AGA-3') and MV2D (5'-CTC AGT CTG TCG GAG GAC TG-3'). The comparability between samples was determined by the electrophoresis of an equal amount (500 ng) of total RNA from each sample.

Cloning and sequencing

Polymerase chain reaction (PCR) products were purified using a Qiaquick PCR Purification kit (Qiagen) and cloned into the pGEM-T Easy vector (Promega, Madison, Wis). Plasmid DNAs for sequencing analysis were prepared using a Qiaprep Spin Miniprep kit (Qiagen). Sequencing was performed at the Molecular Cloning Laboratory (South San Francisco, Calif).

Multiple alignment and phylogenetic analyses

Initially, a total of 53 (41 from sepsis repressed and 12 from sepsis induced) MuERV U3 clones were aligned using Vector NTI (Invitrogen, Carlsbad, Calif) and 35 (31 from sepsis repressed and 4 from sepsis induced) unique U3 clones were identified. The neighbor-joining method within MEGA4 program was used for phylogenetic analysis (25). To evaluate the statistical confidence of branching patterns, bootstrapping was performed with 100 replications within the program. In addition, multiple alignment and phylogenetic analyses of six U3 sequences derived from variant transcripts

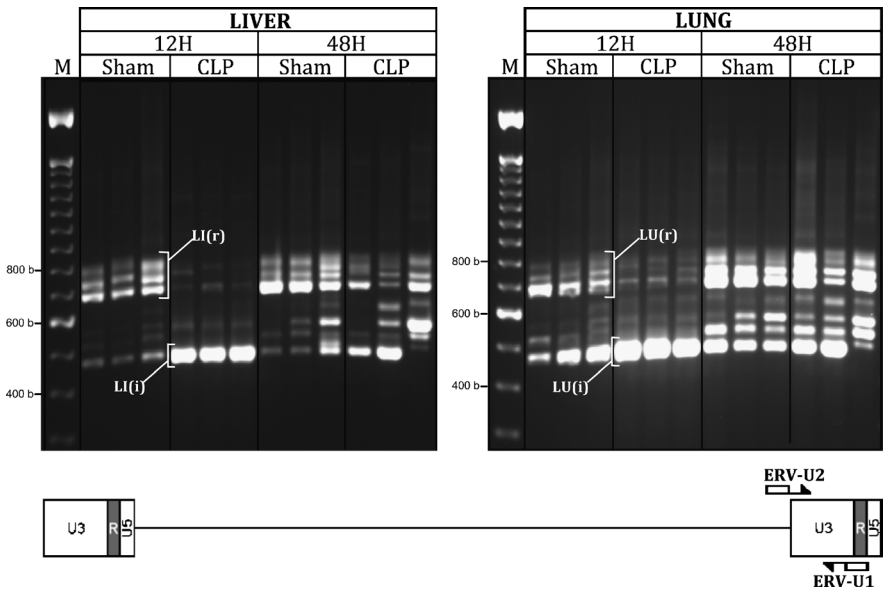


FIG. 1. Changes in profiles of MuERV expression in the liver and lung after CLP. Tissues (liver and lung) harvested at 12 and 48 h after CLP were subjected to RT-PCR analysis of MuERV expression using a primer set flanking the 3' U3 region. Respective tissues harvested from sham mice (same treatment as CLP mice except for CLP procedure) served as controls. A schematic diagram depicts the locations of primers (ERV-U2 and ERV-U1) flanking the 3' U3 region. i indicates (induced); r, (repressed); LI, liver; LU, lung.

and five putative envelope polypeptides were performed, respectively, using the same protocol.

Tropism traits of U3 promoter sequences

The putative tropism traits of 35 unique U3 clones were determined by comparison to the reference sequences (direct repeat, insertion, and unique sequence) first reported by Tomonaga and Coffin (26, 27). A total of five direct repeats (1/1*, 3/3*, 4/4*, 5/5*, and 6/6*), one 190–base pair (bp) insertion, and one unique sequence (2) served as reference sequences for the tropism analysis.

Transcription regulatory elements of U3 promoter sequences

Profiles of transcription regulatory elements on 35 unique U3 clones/promoters were determined using the MatInspector program (Genomatix, Munich, Germany). The core similarity was set to 0.90, and the matrix similarity was optimized within the vertebrate matrix group (28).

Open reading frame analysis

The open reading frames (ORFs) of individual variant transcripts were analyzed using the ORF search feature within Vector NTI (Invitrogen). The parameter was set with “ATG” as the start codon, and each candidate ORF

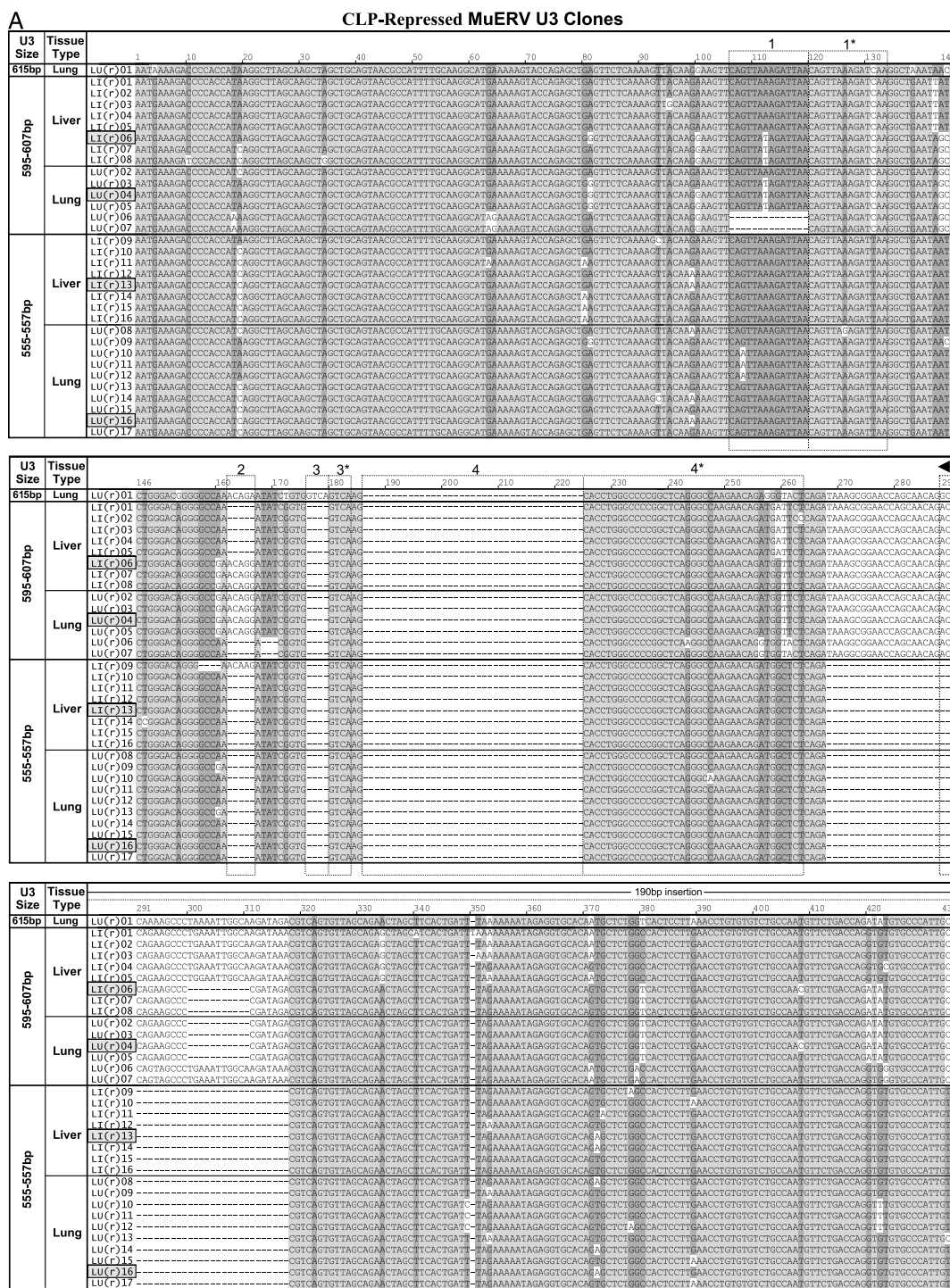


FIG. 2. **Multiple alignment of CLP-repressed and CLP-induced MuERV U3 clones.** A total of 38 CLP-repressed (33) and CLP-induced (5) MuERV U3 clones isolated from the liver and lung were subjected to multiple alignment analysis. Different gray scales and a dash indicate various levels of sequence homology among the sequences aligned (dash: absence of sequence). Distinct sequence features (190-bp insertion, direct repeats, unique sequence, and TATA box) are indicated by a dotted box. Identical U3 clones, which are present in both tissues, are highlighted in gray.

collected at 12 and 48 h after cecal ligation and puncture (CLP) were subjected to reverse transcriptase–polymerase chain reaction (RT-PCR) analysis by amplifying the 3′ U3 regions of MuERV transcripts. The 3′ U3 sequences were amplified because the same sequence on the 5′-end of provirus (5′ U3 sequence) serves as a promoter, and this region is known to be highly polymorphic among the MuERV population compared with the rest. The MuERV profiles of the CLP liver and lung at 12 h were different from the profiles of the sham mice at both 12 and 48 h (Fig. 1). The differentially regulated 3′ U3 regions (repressed [LI(r) and LU(r)] or induced [LI(i) and LU(i)]; Fig. 1) in the liver and lung at

RESULTS

To investigate whether polymicrobial sepsis-elicited stress signals affect MuERV expression, liver and lung tissues



12 h after CLP were cloned for downstream analyses, such as evolutionary relationship, tropism, and transcription potential.

Comparison of MuERV U3 clones isolated from CLP-repressed and CLP-induced U3 fragments

To identify the putative MuERVs and their promoters whose expression was altered in response to CLP-elicited stress signals, we examined the differences in sequences between CLP-repressed and CLP-induced MuERV U3 regions. A total of 53 U3 clones were isolated from four fragments, LI(r), LU(r), LI(i), and LU(i), identified in Figure 1. Alignment analyses identified 17 unique U3 clones in the liver (16 CLP repressed and 1 CLP induced) and 21 unique clones in the lung (17 CLP repressed and 4 CLP induced) (Fig. 2). Among them, three U3 clones (two CLP repressed and one CLP induced) were shared by both liver and lung. The CLP-repressed U3 clones (33 total) ranged from 555 to 615 bp in size, whereas the CLP-induced clones (five total) were of 346 or 347 bp. Interestingly, the 555- to 557-bp U3 sequences were expressed the most in the sham livers at both time points. It needs to be noted that the PCR-amplified U3 regions include the envelope sequence at the 5'-end and R (repeat) sequence at the 3'-end, and these sequences were removed before the U3 alignment analyses. Comparison analyses of the CLP-repressed U3 clones revealed four direct repeats (1/1*, 3/3*, 5/5*, and 6/6*), one unique sequence (2), and one ~190-bp insertion. These sequences were previously described as references for determining tropism traits of MuERVs (27). The direct repeat "4/4*" was not present in any of the CLP-repressed U3 clones, and the size of the ~190-bp insertion was variable. All of the CLP-repressed U3 clones except for the LU(r)06 and LU(r)07 had the direct repeat "1/1*," whereas the direct repeats "3/3*" and "5/5*" were identified only in LU(r)01, LU(r)06 and LU(r)07. In contrast to the CLP-repressed U3 clones, three direct repeats (1/1*, 4/4*, and 6/6*), one unique sequence (2), and no ~190-bp insertion were identified in all CLP-induced U3 clones examined. It is of interest to find the 4/4* direct repeat in all CLP-induced U3 clones, in contrast to its absence in all CLP-repressed U3 clones, whereas direct repeats of 3/3* and 5/5* are present in the CLP repressed but not in the CLP induced.

A phylogenetic tree of both CLP-repressed and CLP-induced U3 clones was established based on the alignment data (Fig. 3). As expected, primarily based on their size differences with regard to the repressed group, the CLP-induced U3 clones were segregated on a unique branch (highlighted in a dotted box). Interestingly, the branching pattern of the CLP-repressed LU(r)06 and LU(r)07 U3 clones was closer to the CLP-induced U3 clones rather than the other CLP-repressed U3 clones. In addition, one distinct branch of five CLP-repressed U3 clones was established from the liver (highlighted in gray) but not the lung.

Tropism traits and transcription potentials of the CLP-repressed and CLP-induced U3 clones

A total of 38 (35 unique) U3 clones isolated from differentially amplified U3 regions were subjected to tropism trait analysis (Table 1). The sequence characteristics, primarily the direct repeat, unique sequence, and ~190-bp insertion, of the

individual U3 clones were surveyed to determine their putative tropism traits. The survey resulted in 29 polytropic and six xenotropic clones (Table 1). Interestingly, among the 31 unique CLP-repressed U3 clones, only two, [LU(r)06 and LU(r)07] clones, were xenotropic, whereas all four CLP-induced clones were xenotropic as well, which parallels the phylogenetic data described above. However, the significance of this *in silico* finding is yet to be determined by further *in vitro* and *in vivo* experiments.

To evaluate the transcription potential of individual U3 promoters/clones identified in this study, the profiles of transcription regulatory elements were determined by mapping the consensus sequences of each element. A total of 83 transcription regulatory elements, including the TATA box and CCAAT enhancer, were identified from the 38 (35 unique) U3 clones examined [Table 2. The transcription regulatory element profiles from the CLP-repressed U3 clones were different from those induced by CLP. Five transcription regulatory elements (column labeled as "A") were present only in U3 clones derived from the CLP repressed, and three (column labeled as "B") were from the CLP induced, whereas four elements (column labeled as "C") were shared by all U3 clones examined].

CLP-mediated changes in expression of MuERV variant transcripts

In this study, we examined how the CLP-elicited stress signals affect the profile of full-length as well as variant MuERV transcripts in the liver and lung. We also identified specific MuERV

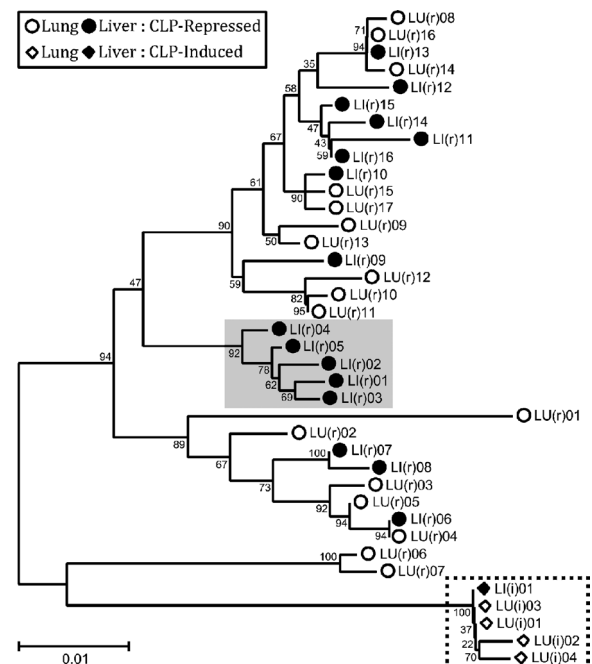


FIG. 3. Phylogenetic analysis of CLP-repressed and CLP-induced MuERV U3 clones. After the multiple alignment analysis, all 38 MuERV U3 clones of CLP repressed and CLP induced were subjected to phylogenetic analysis. The branching pattern of the CLP-induced MuERV U3 clones was unique compared with the pattern of the CLP repressed. The CLP-induced U3 clones segregated on a unique branch are highlighted in a dotted box. In addition, one distinct branch of five CLP-repressed U3 clones isolated from the liver is highlighted in gray. Branch lengths are proportional to the distance between the taxa, which are drawn to scale. The values at the branch nodes indicate the percentage support for a particular branching pattern.

TABLE 1. Summary of tropism traits of CLP-repressed and CLP-induced MuERV U3 clones

	Size	Tissue	U3	Direct Repeat/Unique Region						Tropism
				1/1*	2	3/3*	4/4*	5/5*	6/6*	
				P-I, P-II	P-II, P-III, P-V, X-I, X-II, X-IV	P-II	P-II, P-IV, X-I	P-I, P-II	P-II, X-I	
CLP Repressed	615bp	Liver	LU(r01)	P-I, P-II	P-I, P-IV, X-III	P-I, P-II, P-III, P-IV, X-I, X-IV	P-III	P-I, P-II	P-I, P-II, P-III, X-I, X-II, X-III, X-IV	P-I
			LI(r02)	P-I, P-II	P-I, P-IV, X-III	P-I, P-II, P-III, P-IV, X-I, X-IV	P-III	P-I, P-II	P-I, P-II, P-III, X-I, X-II, X-III, X-IV	P-I
			LI(r03)	P-I, P-II	P-I, P-IV, X-III	P-I, P-II, P-III, P-IV, X-I, X-IV	P-III	P-I, P-II	P-I, P-II, P-III, X-I, X-II, X-III, X-IV	P-I
			LI(r04)	P-I, P-II	P-I, P-IV, X-III	P-I, P-II, P-III, P-IV, X-I, X-IV	P-III	P-I, P-II	P-I, P-II, P-III, X-I, X-II, X-III, X-IV	P-I
			LI(r05)	P-I, P-II	P-I, P-IV, X-III	P-I, P-II, P-III, P-IV, X-I, X-IV	P-III	P-I, P-II	P-I, P-II, P-III, X-I, X-II, X-III, X-IV	P-I
			LI(r06)	P-II	P-II, P-III, P-V, X-I, X-II, X-IV	P-I, P-II, P-III, P-IV, X-I, X-IV	P-II	P-I, P-II	P-II, X-I	P-II
			LI(r07)	P-II	P-II, P-III, P-V, X-I, X-II, X-IV	P-I, P-II, P-III, P-IV, X-I, X-IV	P-II	P-I, P-II	P-I, P-II, P-III, X-I, X-II, X-III, X-IV	P-II
			LI(r08)	P-II	P-II, P-III, P-V, X-I, X-II, X-IV	P-I, P-II, P-III, P-IV, X-I, X-IV	P-II	P-I, P-II	P-I, P-II, P-III, X-I, X-II, X-III, X-IV	P-II
	595-607bp	Liver	LU(r02)	P-I, P-II	P-II, P-III, P-V, X-I, X-II, X-IV	P-I, P-II, P-III, P-IV, X-I, X-IV	P-II	P-I, P-II	P-II, X-I	P-II
			LU(r03)	P-II	P-II, P-III, P-V, X-I, X-II, X-IV	P-I, P-II, P-III, P-IV, X-I, X-IV	P-II	P-I, P-II	P-II, X-I	P-II
			LU(r04)	P-II	P-II, P-III, P-V, X-I, X-II, X-IV	P-I, P-II, P-III, P-IV, X-I, X-IV	P-II	P-I, P-II	P-II, X-I	P-II
			LU(r05)	P-II	P-II, P-III, P-V, X-I, X-II, X-IV	P-I, P-II, P-III, P-IV, X-I, X-IV	P-II	P-I, P-II	P-II, X-I	P-II
			LU(r06)	X-IV	P-I, P-IV, X-III	P-I, P-II, P-III, P-IV, X-I, X-IV	X-I	X-II, X-III, X-IV	P-I, P-II, P-III, X-I, X-II, X-III, X-IV	X-IV
			LU(r07)	X-IV	P-I, P-IV, X-III	P-I, P-II, P-III, P-IV, X-I, X-IV	X-I	X-II, X-III, X-IV	P-I, P-II, P-III, X-I, X-II, X-III, X-IV	X-IV
			LI(r09)	P-I	P-II, P-III, P-V, X-I, X-II, X-IV	P-I, P-II, P-III, P-IV, X-I, X-IV	P-I	P-I, P-II, P-III	P-II, X-I	P-I
			LI(r10)	P-I	P-I, P-IV, X-III	P-I, P-II, P-III, P-IV, X-I, X-IV	P-I	P-I, P-II, P-III	P-I, P-II, P-III, X-I, X-II, X-III, X-IV	P-I
	595-607bp	Liver	LI(r11)	P-I	P-I, P-IV, X-III	P-I, P-II, P-III, P-IV, X-I, X-IV	P-I	P-I, P-II, P-III	P-I, P-II, P-III, X-I, X-II, X-III, X-IV	P-I
			LI(r12)	P-I	P-I, P-IV, X-III	P-I, P-II, P-III, P-IV, X-I, X-IV	P-I	P-I, P-II, P-III	P-I, P-II, P-III, X-I, X-II, X-III, X-IV	P-I
			LI(r13)	P-I	P-I, P-IV, X-III	P-I, P-II, P-III, P-IV, X-I, X-IV	P-I	P-I, P-II, P-III	P-I, P-II, P-III, X-I, X-II, X-III, X-IV	P-I
			LI(r14)	P-I	P-I, P-IV, X-III	P-I, P-II, P-III, P-IV, X-I, X-IV	P-I	P-I, P-II, P-III	P-I, P-II, P-III, X-I, X-II, X-III, X-IV	P-I
			LI(r15)	P-I	P-I, P-IV, X-III	P-I, P-II, P-III, P-IV, X-I, X-IV	P-I	P-I, P-II, P-III	P-I, P-II, P-III, X-I, X-II, X-III, X-IV	P-I
			LI(r16)	P-I	P-I, P-IV, X-III	P-I, P-II, P-III, P-IV, X-I, X-IV	P-I	P-I, P-II, P-III	P-I, P-II, P-III, X-I, X-II, X-III, X-IV	P-I
			LU(r08)	P-I	P-I, P-IV, X-III	P-I, P-II, P-III, P-IV, X-I, X-IV	P-I	P-I, P-II, P-III	P-I, P-II, P-III, X-I, X-II, X-III, X-IV	P-I
			LU(r09)	P-I	P-I, P-IV, X-III	P-I, P-II, P-III, P-IV, X-I, X-IV	P-I	P-I, P-II, P-III	P-I, P-II, P-III, X-I, X-II, X-III, X-IV	P-I
CLP Induced	595-607bp	Liver	LU(r10)	P-I	P-I, P-IV, X-III	P-I, P-II, P-III, P-IV, X-I, X-IV	P-I	P-I, P-II, P-III	P-I, P-II, P-III, X-I, X-II, X-III, X-IV	P-I
			LU(r11)	P-I	P-I, P-IV, X-III	P-I, P-II, P-III, P-IV, X-I, X-IV	P-I	P-I, P-II, P-III	P-I, P-II, P-III, X-I, X-II, X-III, X-IV	P-I
			LU(r12)	P-I	P-I, P-IV, X-III	P-I, P-II, P-III, P-IV, X-I, X-IV	P-I	P-I, P-II, P-III	P-I, P-II, P-III, X-I, X-II, X-III, X-IV	P-I
			LU(r13)	P-I	P-I, P-IV, X-III	P-I, P-II, P-III, P-IV, X-I, X-IV	P-I	P-I, P-II, P-III	P-I, P-II, P-III, X-I, X-II, X-III, X-IV	P-I
			LU(r14)	P-I	P-I, P-IV, X-III	P-I, P-II, P-III, P-IV, X-I, X-IV	P-I	P-I, P-II, P-III	P-I, P-II, P-III, X-I, X-II, X-III, X-IV	P-I
			LU(r15)	P-I	P-I, P-IV, X-III	P-I, P-II, P-III, P-IV, X-I, X-IV	P-I	P-I, P-II, P-III	P-I, P-II, P-III, X-I, X-II, X-III, X-IV	P-I
			LU(r16)	P-I	P-I, P-IV, X-III	P-I, P-II, P-III, P-IV, X-I, X-IV	P-I	P-I, P-II, P-III	P-I, P-II, P-III, X-I, X-II, X-III, X-IV	P-I
			LU(r17)	P-I	P-I, P-IV, X-III	P-I, P-II, P-III, P-IV, X-I, X-IV	P-I	P-I, P-II, P-III	P-I, P-II, P-III, X-I, X-II, X-III, X-IV	P-I
		Lung	LU(r01)	X-II, X-III	P-II, P-III, P-V, X-I, X-II, X-IV	.	X-II, X-IV	.	P-I, P-II, P-III, X-I, X-II, X-III, X-IV	X-II
			LU(r01)	X-II, X-III	P-II, P-III, P-V, X-I, X-II, X-IV	.	X-II, X-IV	.	P-I, P-II, P-III, X-I, X-II, X-III, X-IV	X-II
			LU(r02)	X-II, X-III	P-II, P-III, P-V, X-I, X-II, X-IV	.	X-II, X-IV	.	P-I, P-II, P-III, X-I, X-II, X-III, X-IV	X-II
			LU(r03)	X-II, X-III	P-II, P-III, P-V, X-I, X-II, X-IV	.	X-II, X-IV	.	P-I, P-II, P-III, X-I, X-II, X-III, X-IV	X-II
			LU(r04)	X-II, X-III	P-II, P-III, P-V, X-I, X-II, X-IV	.	X-II, X-IV	.	P-I, P-II, P-III, X-I, X-II, X-III, X-IV	X-II
			LU(r04)	X-II, X-III	P-II, P-III, P-V, X-I, X-II, X-IV	.	X-II, X-IV	.	P-I, P-II, P-III, X-I, X-II, X-III, X-IV	X-II

Dot indicates absence of homology with reference sequences. Bold font represents the reference type closest to each U3 clone examined. Identical U3 clones, which are present in both liver and lung, are highlighted in gray.

variant transcripts responding to the stress signals. Reverse transcriptase–polymerase chain reaction analyses using a set of primers that are capable of amplifying full-length MuERV as well as subgenomic transcripts revealed that several variant transcripts were regulated in the liver and lung in response to CLP (Fig. 4). However, we were not able to detect any full-length transcripts, presumably ~7.5 to ~8 kb in size, in any experimental groups examined. There were unique and substantial changes in variant transcripts in the liver at 12 h (LI-C1_(12H), LI-C2_(12H), LI-C3_(12H), and LI-C4_(12H)) compared with changes in the liver and lung at 48 h (LI-S1_(48H), LI-S2_(48H), LI-C1_(48H), and LU-C1_(48H)). Four different sizes of variant transcripts (~5 kb [LI-C1_(12H)], ~2.3 kb [LI-C2_(12H)], ~1.2 kb [LI-C3_(12H)], and ~0.9 kb [LI-C4_(12H)]) were induced in the liver at 12 h after CLP, whereas only the ~0.9-kb transcript was induced in the lung. In contrast, at 48 h after CLP, a variant transcript of ~2.8 kb (LI-C1_(48H)/ LI-S1_(48H)), which is about the size of the typical MuERV envelope transcript, was induced in two of three CLP mice, and one variant transcript of ~1.5 kb (LU-C1_(48H)) was induced in the lung (two of three mice). Another envelope size variant transcript (~2.9 kb [LI-S2_(48H)]) was present in the livers of two sham mice at 48 h, but it was not detected in any of the CLP mice.

Characterization of splicing patterns and coding potentials of CLP-associated MuERV variant transcripts

To determine the splicing patterns of the variant transcripts identified above, each transcript cloned from the amplified products (indicated in Fig. 4) was examined for splicing

junctions. In addition, coding potentials of these variant transcripts were evaluated for three retroviral genes (group specific antigen [*gag*], polymerase [*pol*], and envelope [*env*]) essential for viral replication. Four near-identical (>99% sequence identity) transcripts (5,063 or 5,064 bp) were cloned from the LI-C1_(12H) fragment. There were four ORFs (I ~ IV) in these transcripts, and none were intact for any of the three main retroviral polypeptides (*gag*, *pol*, and *env*) (Fig. 5). Interestingly, a single-nucleotide deletion in one clone led to a premature termination of ORF III. Putative splicing junctions were surveyed in these transcripts using the reference sequences for splice donors (S/D) and splice acceptors (S/A) yielding a negative result, suggesting that the transcripts are nonsplicing variants (NSVs) transcribed from defective MuERV provirus(es) (19, 29). In fact, a BLAST search of the C57BL/6J genome using one of these transcripts revealed two genomic loci in chromosomes 4 and 8 with more than 99.9% sequence identity with one nucleotide gap and no gap, respectively.

It has been documented that the U3 promoters are highly polymorphic and are the primary determinants of MuERV transcriptional activity and tropism (27). Comparison analysis of the U3 promoter sequences of all variant transcripts identified in this study revealed that all transcripts induced at 12 h in the liver (LI-C1_(12H), LI-C2_(12H), LI-C3_(12H), and LI-C4_(12H)) share more than 99% sequence identity within their U3 sequences of 346-bp size (Fig. 6). In contrast, four different sizes (434, 556, 600, and 611 bp) of U3 promoters were found in the transcripts isolated from the liver and lung at 48 h

TABLE 2. Profiles of transcription regulatory elements in the CLP-repressed and CLP-induced MuERV U3 promoters

CTD Element	CTD Element Size	Tissue Type	Source	Transcription Regulatory Element	
				CTD Element Size	Source
615bp	Lung	UT(r)01			
		UT(r)02			
		UT(r)03			
		UT(r)04			
		UT(r)05			
		UT(r)06			
	Liver	UT(r)07			
		UT(r)08			
		UT(r)09			
		UT(r)10			
		UT(r)11			
		UT(r)12			
995-607bp	Lung	UT(r)13			
		UT(r)14			
		UT(r)15			
		UT(r)16			
		UT(r)17			
		UT(r)18			
	Liver	UT(r)19			
		UT(r)20			
		UT(r)21			
		UT(r)22			
		UT(r)23			
		UT(r)24			
555-557bp	Lung	UT(r)25			
		UT(r)26			
		UT(r)27			
		UT(r)28			
		UT(r)29			
		UT(r)30			
	Liver	UT(r)31			
		UT(r)32			
		UT(r)33			
		UT(r)34			
		UT(r)35			
		UT(r)36			
346-347bp	Liver	UT(r)37			
		UT(r)38			
		UT(r)39			
		UT(r)40			
		UT(r)41			
		UT(r)42			
	Lung	UT(r)43			
		UT(r)44			
		UT(r)45			
		UT(r)46			
		UT(r)47			
		UT(r)48			

Numbers in the boxes indicate frequency of each element. Different letters in combination with gray shades indicate elements mapped only in U3 clones of CLP repressed (A), only in U3 clones of CLP induced (B), or shared by all U3 clones (C). Identical U3 clones, which are present in both liver and lung, are highlighted in gray.

(LI-S1_(48H), LI-S2_(48H), LI-C1_(48H), and LU-C1_(48H)). Alignment analyses of variant transcripts of LI-C1_(12H), LI-C2_(12H), LI-C3_(12H), and LI-C4_(12H) revealed more than 99% identity within the overlapping sequences among them. We then examined whether the variant transcripts are splicing products derived from the transcripts of LI-C1_(12H). The variant

transcripts were surveyed for potential splicing junctions using reference sequences (Fig. 5) (19, 29). Five different splicing variants (SVs) were identified from the transcripts isolated from the liver at 12 h, and they are presumed to be the splicing products of the 5,063- and/or 5,064-bp NSV transcripts using combinations of previously described as well as novel

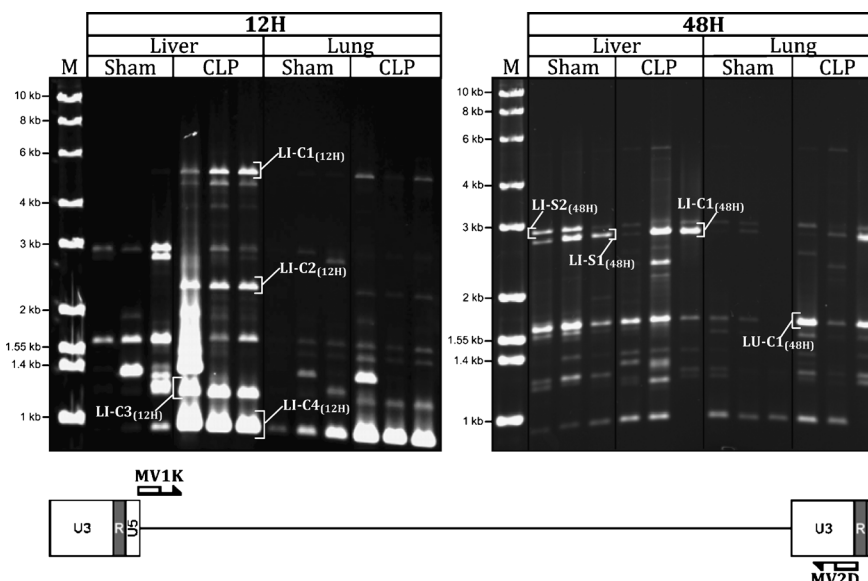


FIG. 4. Changes in profiles of MuERV variant transcripts in the liver and lung after CLP. Liver and lung tissues harvested at 12 and 48 h after CLP were examined for expression of MuERV variant transcripts using a primer set capable of amplifying full-length MuERV transcripts. Several MuERV variant transcripts, including ~1- to 5-kb band, were differentially expressed after CLP. Respective tissues harvested from sham mice served as controls. A schematic drawing depicts the locations of the primers (MV1K and MV2D) used for this experiment. S indicates sham; C, CLP.

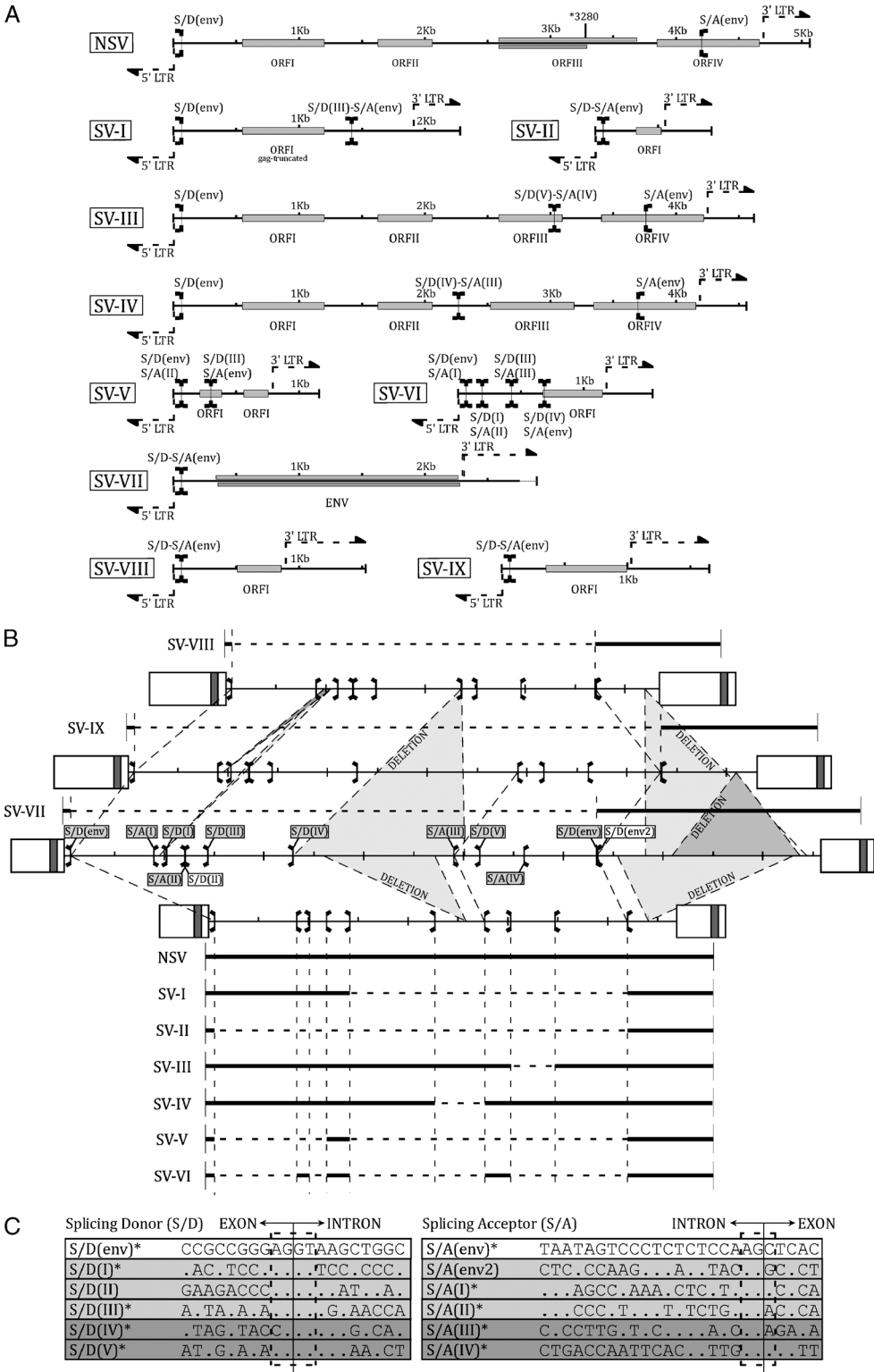


FIG. 5. Genetic organization of CLP-associated MuERV variant transcripts. A, Genetic organization, including putative ORFs, of 10 different types of CLP-associated MuERV variant transcripts (NSV and SV-I to SV-IX) is schematically presented. Each type of variant transcript is drawn on a scaled line on which splicing signals (left bracket [donor] and right bracket [acceptor]) and putative ORFs (gray box) are indicated. Different gray scales were used when more than one putative ORF was identified in the same coding region. Also, 3'-end of 5' LTR and 5'-end of 3' LTR are marked. B, Splicing profiles of nine MuERV variant transcripts are summarized and compared with each other. Based on the sequence homology with individual groups of variant transcripts, three defective MuERVs identified from the C57BL/6J genome and one full-length reference, xenotropic MuERV (DQ241301), were used as references on which splicing signals are indicated. In addition, deletions within three defective reference MuERVs are delineated with gray shades. C, A total of 10 splicing signals (five donors and five acceptors marked with “*”), which were differentially used to generate the SVs identified in this study, are summarized and compared with previously reported signals. Four of them [two donors, S/D(IV) and S/D(V), and two acceptors, S/A(III) and S/A(IV)] highlighted in a darker shade were novel splicing signals and were well conserved, including 100% compliance with the “GT-AG” rule.

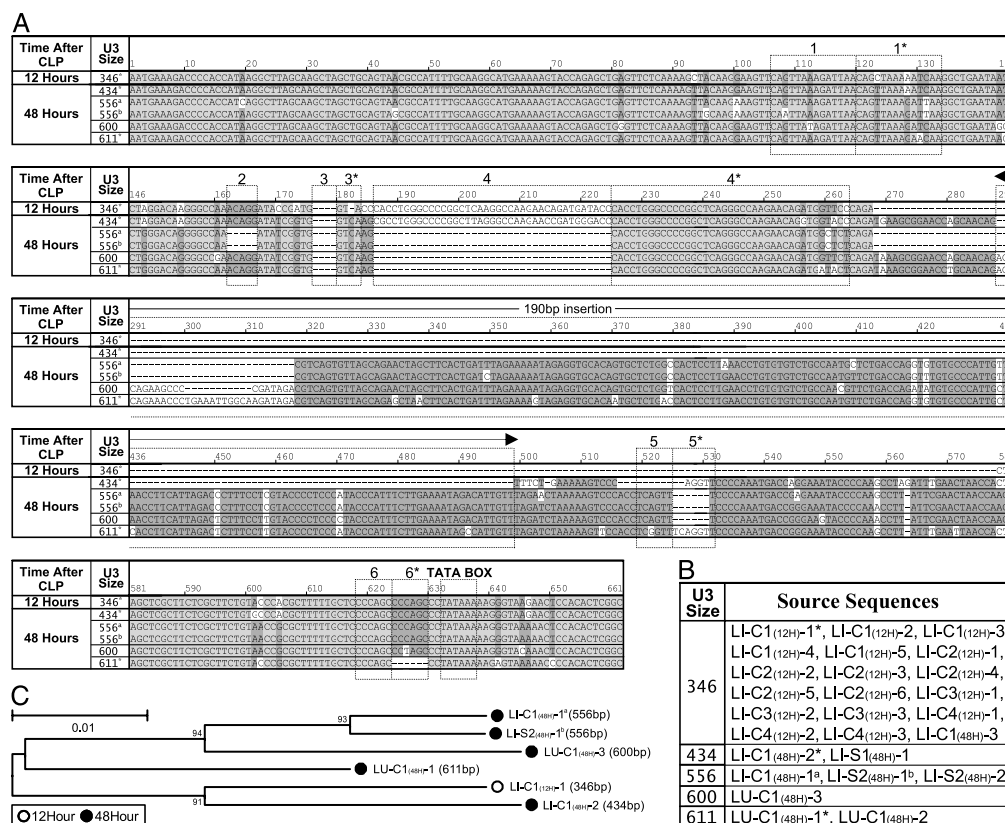


FIG. 6. Comparison analyses of U3 sequences derived from CLP-associated MuERV variant transcripts. A, A total of six different U3 sequences representing the CLP-associated MuERV variant transcripts (LI-C1(12h), LI-C2(12h), LI-C3(12h), LI-C4(12h), LI-C1(48h), LI-S1(48h), and LU-C1(48h)) were subjected to multiple alignment analysis. The LI-C1(12h)-1 U3 sequence is shared by all transcripts from the 12-h time point (LI-C1(12h), LI-C2(12h), LI-C3(12h), and LI-C4(12h)) with a greater than 99% sequence identity. B, The variant transcripts that share a greater than 99% sequence identity with the individual U3 sequences (marked with *, ^a, or ^b), which were subjected to an alignment analysis above, are listed in a table. C, Based on the alignment data, a phylogenetic tree was established using the neighbor-joining method. The U3 sequence (LI-C1(12h)-1) representing all transcripts from 12 h and LI-C1(48h)-2 shared a unique branching pattern. The values at the branch nodes indicate the percentage support for a particular branching pattern.

splicing signals. There was a single splicing event in four variants (SV-I [S/D(III)-S/A(env)], SV-II [S/D(env)-S/A(env)], SV-III [S/D(V)-S/A(IV)], and SV-IV [S/D(IV)-S/A(III)]) and two events in one variant (SV-V [S/D(env)-S/A(II)] and S/D(III)-S/A(env)). Interestingly, one of the variant transcripts identified in the CLP liver at 48 h, called SV-VI, had more than 99% identity within the overlapping sequences with the above variants (SV-I ~ SV-V) and was generated by four splicing events [S/D(env)-S/A(I), S/D(I)-S/A(II), S/D(III)-S/A(III), S/D(V)-S/A(env)]. None of these SVs (SV-I ~ SV-VI) were able to encode intact polypeptides of *gag*, *pol*, or *env*.

Sequence analysis and splicing survey of the variant transcripts of ~2.8 to ~2.9 kb from the liver at 48 h (LI-S1(48h), LI-S2(48h), and LI-C1(48h)) yielded five different full-length *env* transcripts (SV-VII [env/env]) (Fig. 6). In addition, the variant transcripts isolated from the CLP lung at 48 h (LU-C1(48h)) were determined to be two different defective *env* transcripts (SV-VIII and SV-IX) derived from at least two different MuERV loci on the genome that have major deletions in the *env* and/or other genes (Fig. 5). Two defective MuERVs presumed to be proviral templates for SV-VIII and SV-IX were mapped on chromosomes 11 and 13 of the C57BL/6J genome with 94% and 100% sequence identity within the relevant U3 sequences, respectively.

The splicing signals used to generate the variant transcripts identified in this study are summarized in Figure 5C. In addition to the *env* S/D and S/A, eight well-conserved MuERV splicing signals (four donors [S/D(I), S/D(III), S/D(IV), and S/D(V)] and four acceptors [S/A(I), S/A(II), S/A(III), and S/A(IV)]) were used in combinations to generate the variant transcripts. Four [S/D(IV), S/D(V), S/A(III), and S/A(IV)] of these splicing signals have not been reported previously, whereas the other four signals [S/D(I), S/D(III), S/A(I), and S/A(II)] were identified in one of our previous burn studies (19, 29).

Comparison of MuERV U3 sequences of the variant transcripts differentially expressed after CLP

To determine the relationships among the MuERVs from which the variant transcripts were derived, their U3 sequences were compared, and a phylogenetic tree was established (Fig. 6). A 346-bp U3 sequence was shared by a total of the initial 18 variant transcripts cloned, which include all clones (SV-I ~ SV-V) from the CLP liver at 12 h and one (SV-VI) from the CLP liver at 48 h with greater than 99% sequence identity. This 346-bp U3 sequence, which was mostly derived from the CLP-induced variant transcripts at 12 h, was almost identical (>99% sequence identity) to the CLP-induced U3 clones (Fig. 2). Two full-length *env* transcripts (LI-C1(48h)-2

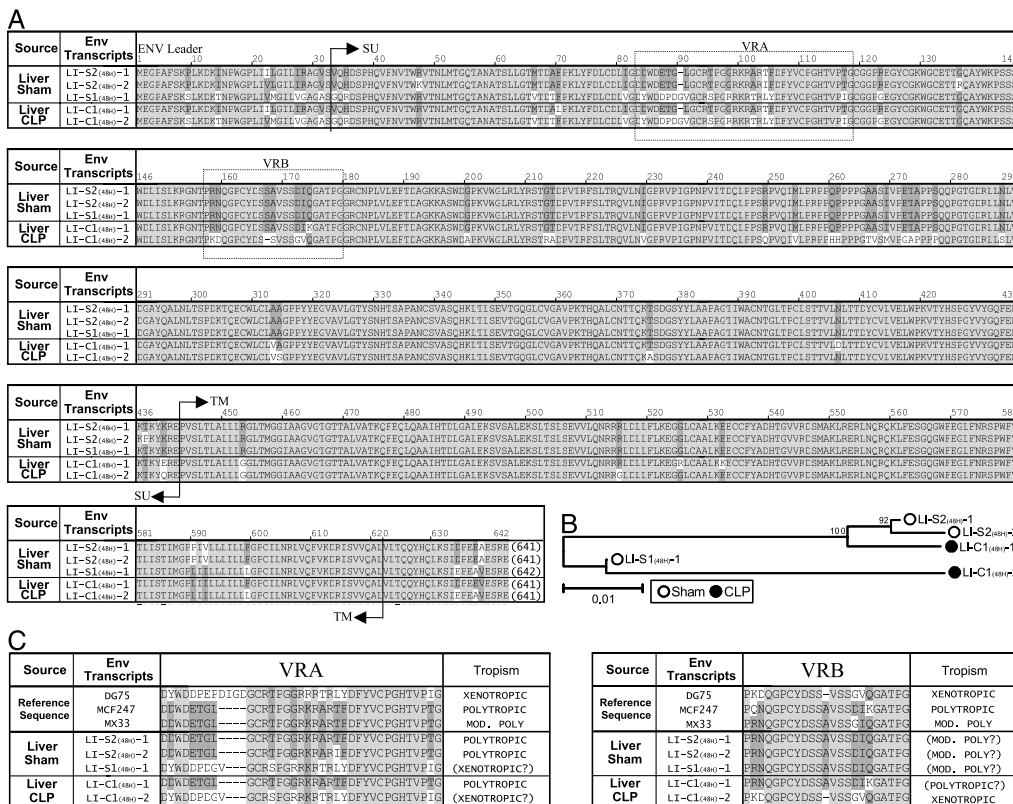


Fig. 7. Comparison of putative *env* polypeptides isolated from the liver of CLP and sham mice at 48 h. A and B, Putative *env* polypeptide sequences encoded from five different *env* transcripts of the SV-VII were compared with reference sequences of different tropism traits by multiple alignment analysis, and a phylogenetic tree was established based on the alignment data (30). Different regions (leader peptide, surface domain [SU], transmembrane domain [TM], variable region A [VRA], and variable region B [VRB]) within the *env* polypeptides are indicated. C, In addition, tropism traits of these putative *env* polypeptides were determined using reference *env* polypeptides with previously known tropism (30).

and LI-S1_(48h)-1 of SV-VII had a 434-bp U3 sequence with one nucleotide difference between each other, whereas the other three members of SV-VII (LI-C1_(48h)-1, LI-S2_(48h)-1, and LI-S2_(48h)-2) shared a 556-bp U3 sequence (two identical plus one with 11-nucleotide mismatch). In addition, there were two SV-VIII transcripts (LI-C1_(48h)-1, LI-C1_(48h)-2) sharing a 611-bp U3 sequence with greater than 99% sequence identity (four nucleotides mismatch), and SV-IX was represented by one transcript (LI-C1_(48h)-3) with a 600-bp U3 sequence. Interestingly, phylogenetic analysis of the U3 sequences of all SVs (SV-I ~ SV-IX) revealed that two members of SV-VII retaining a 434-bp U3 sequence were evolutionarily closer to NSV and SV-I ~ SV-VI with a 346-bp U3 than they were to the other three SV-VII members, SV-VIII, and SV-IX (Fig. 6). The direct repeat 4/4* was present only in two U3 sequences of 346 and 434 bp, suggesting their unique tropism traits.

Putative *env* polypeptides encoded from CLP-associated, full-length *env* transcripts

Five different full-length *env* transcripts of SV-VII isolated in the liver of sham and/or CLP mice were translated. Their polypeptide sequences were subjected to multiple alignment and phylogenetic analyses (Fig. 7). Two *env* polypeptides encoded from *env* transcripts of LI-C1_(48h)-2 and LI-S1_(48h)-1 were placed on one main branch, whereas the other three (LI-C1_(48h)-1, LI-S2_(48h)-1, and LI-S2_(48h)-2) segregated together into another branch. It is likely that the *env* polypeptides

encoded from LI-C1_(48h)-2 and LI-S1_(48h)-1 transcripts (either or both) were induced in the CLP liver at 48 h (Fig. 4). In addition, the tropism traits of these *env* polypeptides were determined by comparison to the variable regions A and B (VRA and VRB) of reference sequences (Fig. 7) (30). Comparison analysis using VRA sequences revealed that three (LI-C1_(48h)-1, LI-S2_(48h)-1, and LI-S2_(48h)-2) were presumed to be polytropic and two (LI-C1_(48h)-2 and LI-S1_(48h)-1) were close to being xenotropic. However, the results from the VRB were not clear enough to interpret except for the LI-C1_(48h)-2 as xenotropic, probably because of a limited size of the sequences to be aligned. All the other variant transcripts (SV-II, SV-VIII, and SV-IX) with an *env* splicing junction retained only coding potentials for truncated *env* polypeptides.

DISCUSSION

The complex network of signaling events underlying the pathogenesis of sepsis is often unique for individual patients, and it has not been fully understood even after extensive investigations involving a range of molecules and pathways (5, 31, 32). In this study, we examined whether the expression of MuERVs is altered in response to sepsis-elicited stress signals. The key findings are as follows. First, there were substantial changes in the expression of certain MuERVs in the liver and lung of CLP-sepsis mice. Second, individual U3 promoter sequences of CLP-sepsis-regulated MuERVs had

unique characteristics in regard to tropism traits and transcription regulatory elements. In addition, the findings from the phylogenetic analysis suggest that some MuERVs responding to the CLP-elicited stress signals share similar promoter sequences. Third, several MuERV SVs (SV-I ~ SV-IX) were differentially regulated in the liver and lung after CLP. Fourth, among the five full-length *env* transcripts, two of them (LI-C1_(48H)-2 and LI-S1_(48H)-1 of SV-VII) were presumed to be induced in the liver at 48 h after CLP.

All of the variant transcripts whose expression was induced at 12 h after CLP shared a 346-bp U3 promoter (with >99% sequence identity), and they were presumed to be splicing products processed from a variant transcribed from a defective MuERV. In contrast, at 48 h after CLP, four different sizes of U3 promoters (434, 556, 600, and 611 bp) were involved in changes in the expression profile of variant transcripts. The differential usage of MuERV U3 promoters at 12 and 48 h after CLP might be closely linked to the formulation of a unique transcriptional environment at each time point. In particular, it would be important to identify the transcription factors and components of the splicing machinery responsible for the changes in MuERV expression after CLP.

Coincidentally, the two genomic MuERV loci presumed to be proviral templates for CLP-sepsis-induced transcripts (5,063- and 5,064-bp NSVs from ICR stock mice) were shared by a transcript, which was induced in the liver of C57BL/6J mice after burn injury (20). Interestingly, these two different types of stressors (sepsis and burn) influenced the transcription, including splicing, of one specific MuERV (two genomic loci) out of the numerous MuERV copies on the genome. Furthermore, CLP-sepsis and burn experiments were performed in mice with two different backgrounds, ICR and C57BL/6J, respectively (19, 20). The sepsis and burn-associated profiles of the transcriptional environment and epigenetic modification in the liver were presumed to be specific enough to control the MuERV's U3 promoter. In addition, it might be interesting to examine whether MuERV regulation after CLP-sepsis and/or burn at these genomic loci is linked to the expression of neighboring host genes.

Murine endogenous retroviruses have been regarded as simple retroviruses primarily because of limited diversity in their ORFs associated with splicing potentials compared with the complex retroviruses with several splicing events and resulting ORFs. Only two splicing signals (*env* S/D and S/A) were previously known for MuERVs until five additional signals (three donors and two acceptors) were reported from our laboratory, and four novel splicing signals (two donors and two acceptors) are identified in this study (19, 29). These findings suggest that the genomic organization of MuERVs, in regard to splicing and coding potentials, is more complex than previously thought. It might be interesting to investigate the underlying mechanisms of how the stress signals from CLP-sepsis influence the differential splicing events of MuERVs.

There are three potential mechanisms of how certain MuERVs contribute to the pathogenic processes of CLP-sepsis. First, MuERVs encode viral proteins such as *env* and *gag* polypeptides that could participate in CLP-sepsis-associated signaling events. Second, MuERVs may retain coding potentials required for the

assembly of pathogenic virions, resulting in infection into susceptible host cells, such as hepatocytes and alveolar epithelial cells, accompanied by pathological effects. Third, changes in the transcriptional activities of MuERV loci on the genome may influence the expression of neighboring genes, leading to phenotypic alterations in affected cells and tissues.

The results from our preliminary study demonstrated that overexpression of certain MuERV *env* proteins in a macrophage cell line induced differential expression of a few inflammatory mediators (e.g., COX-2, IL-6) (data not shown). These findings may suggest that the CLP-sepsis-activated MuERVs in Kupffer cells and/or alveolar macrophages may participate in a cascade of signaling events associated with early inflammatory response in the liver and lung, respectively. It is likely that the MuERV expression levels will return to normal within 1 week; however, it will be interesting to investigate the long-term pathological effects of infection and genomic random reintegration of the CLP-activated MuERVs.

The CLP-activated MuERVs may exert deleterious and/or beneficial effects during the course of sepsis. One potential positive outcome from the treatment of CLP-sepsis mice with antiretroviral agents (e.g., reverse transcriptase inhibitor, siRNA against *env* gene) will be alleviation of the inflammatory response by reducing the production of inflammatory cytokines.

The findings from this study suggest that the stress signals from CLP-sepsis affect the expression and splicing of specific MuERVs. It may lead to a justification for further investigation into the roles of MuERVs and their gene products in the complex network of pathogenic processes of sepsis.

ACKNOWLEDGMENTS

The authors thank the staff of Minnesota Molecular Inc (Minneapolis, Minn) for the generous gift of molecular weight markers.

REFERENCES

- Angus DC, Wax RS: Epidemiology of sepsis: an update. *Crit Care Med* 29:S109-S116, 2001.
- Bernard GR, Vincent JL, Laterre PF, LaRosa SP, Dhainaut JF, Lopez-Rodriguez A, Steingrub JS, Garber GE, Helterbrand JD, Ely EW, et al.: Efficacy and safety of recombinant human activated protein C for severe sepsis. *N Engl J Med* 344:699-709, 2001.
- Rivers E, Nguyen B, Havstad S, Ressler J, Muzzin A, Knoblich B, Peterson E, Tomlanovich M: Early goal-directed therapy in the treatment of severe sepsis and septic shock. *N Engl J Med* 345:1368-1377, 2001.
- Angele MK, Schwacha MG, Ayala A, Chaudry IH: Effect of gender and sex hormones on immune responses following shock. *Shock* 14:81-90, 2000.
- De Maio A, Torres MB, Reeves RH: Genetic determinants influencing the response to injury, inflammation, and sepsis. *Shock* 23:11-17, 2005.
- Kahlke V, Angele MK, Ayala A, Schwacha MG, Cioffi WG, Bland KI, Chaudry IH: Immune dysfunction following trauma-haemorrhage: influence of gender and age. *Cytokine* 12:69-77, 2000.
- De Maio A, Mooney ML, Matesic LE, Paidas CN, Reeves RH: Genetic component in the inflammatory response induced by bacterial lipopolysaccharide. *Shock* 10:319-323, 1998.
- Garred P, J Strom JS, Quist L, Taaning E, Madsen HO: Association of mannose-binding lectin polymorphisms with sepsis and fatal outcome, in patients with systemic inflammatory response syndrome. *J Infect Dis* 188: 1394-1403, 2003.
- Saleh M, Vaillancourt JP, Graham RK, Huyck M, Srinivasula SM, Alnemri ES, Steinberg MH, Nolan V, Baldwin CT, Hotchkiss RS, et al.: Differential modulation of endotoxin responsiveness by human caspase-12 polymorphisms. *Nature* 429:75-79, 2004.
- Stuber F, Petersen M, Bokelmann F, Schade U: A genomic polymorphism within the tumor necrosis factor locus influences plasma tumor necrosis

- factor- α concentrations and outcome of patients with severe sepsis. *Crit Care Med* 24:381–384, 1996.
11. de Parseval N, Heidmann T: Human endogenous retroviruses: from infectious elements to human genes. *Cytogenet Genome Res* 110:318–332, 2005.
 12. Ramirez MA, Pericuesta E, Fernandez-Gonzalez R, Moreira P, Pintado B, Gutierrez-Adan A: Transcriptional and post-transcriptional regulation of retrotransposons IAP and MuERV-L affect pluripotency of mice ES cells. *Reprod Biol Endocrinol* 4:55–66, 2006.
 13. Reiss D, Mager DL: Stochastic epigenetic silencing of retrotransposons: does stability come with age? *Gene* 390:130–135, 2007.
 14. Bannert N, Kurth R: Retroelements and the human genome: new perspectives on an old relation. *Proc Natl Acad Sci U S A* 101(Suppl 2):14572–14579, 2004.
 15. Mayer J, Sauter M, Racz A, Scherer D, Mueller-Lantzsch N, Meese E: An almost-intact human endogenous retrovirus K on human chromosome 7. *Nat Genet* 21:257–258, 1999.
 16. Mueller-Lantzsch N, Sauter M, Weiskircher A, Kramer K, Best B, Buck M, Grasser F: Human endogenous retroviral element K10 (HERV-K10) encodes a full-length gag homologous 73-kDa protein and a functional protease. *AIDS Res Hum Retroviruses* 9:343–350, 1993.
 17. Antony JM, Ellestad KK, Hammond R, Imaizumi K, Mallet F, Warren KG, Power C: The human endogenous retrovirus envelope glycoprotein, syncytin-1, regulates neuroinflammation and its receptor expression in multiple sclerosis: a role for endoplasmic reticulum chaperones in astrocytes. *J Immunol* 179:1210–1224, 2007.
 18. Antony JM, van Marle G, Opii W, Butterfield DA, Mallet F, Yong VW, Wallace JL, Deacon RM, Warren K, Power C: Human endogenous retrovirus glycoprotein-mediated induction of redox reactants causes oligodendrocyte death and demyelination. *Nat Neurosci* 7:1088–1095, 2004.
 19. Cho K, Adamson LK, Greenhalgh DG: Induction of murine AIDS virus-related sequences after burn injury. *J Surg Res* 104:53–62, 2002.
 20. Cho K, Greenhalgh DG: Injury-associated induction of two novel and replication-defective murine retroviral RNAs in the liver of mice. *Virus Res* 93:189–198, 2003.
 21. Conrad B, Weissmahr RN, Boni J, Arcari R, Schupbach J, Mach B: A human endogenous retroviral superantigen as candidate autoimmune gene in type I diabetes. *Cell* 90:303–313, 1997.
 22. Karlsson H, Bachmann S, Schroder J, McArthur J, Torrey EF, Yolken RH: Retroviral RNA identified in the cerebrospinal fluids and brains of individuals with schizophrenia. *Proc Natl Acad Sci U S A* 98:4634–4639, 2001.
 23. Talal N, Garry RF, Schur PH, Alexander S, Dauphinee MJ, Livas IH, Ballester A, Takei M, Dang H: A conserved idotype and antibodies to retroviral proteins in systemic lupus erythematosus. *J Clin Invest* 85:1866–1871, 1990.
 24. Nemzek JA, Ebong SJ, Kim J, Bolgos GL, Remick DG: Keratinocyte growth factor pretreatment is associated with decreased macrophage inflammatory protein-2 α concentrations and reduced neutrophil recruitment in acid aspiration lung injury. *Shock* 18:501–506, 2002.
 25. Kumar S, Tamura K, Nei M: MEGA3: integrated software for molecular evolutionary genetics analysis and sequence alignment. *Brief Bioinform* 5:150–163, 2004.
 26. Tomonaga K, Coffin JM: Structure and distribution of endogenous non-retroviral murine leukemia viruses in wild mice. *J Virol* 72:8289–8300, 1998.
 27. Tomonaga K, Coffin JM: Structures of endogenous nonretroviral murine leukemia virus (MLV) long terminal repeats in wild mice: implication for evolution of MLVs. *J Virol* 73:4327–4340, 1999.
 28. Quandt K, Frech K, Karas H, Wingender E, Werner T: MatInd and MatInspector: new fast and versatile tools for detection of consensus matches in nucleotide sequence data. *Nucleic Acids Res* 23:4878–4884, 1995.
 29. Cho K, Pham TN, Chamberlain T, Boonyaratankornkit J, Greenhalgh DG: CD14-mediated alterations in transcription and splicing of endogenous retroviruses after injury. *Arch Virol* 149:2215–2233, 2004.
 30. Battini JL, Heard JM, Danos O: Receptor choice determinants in the envelope glycoproteins of amphotropic, xenotropic, and polytropic murine leukemia viruses. *J Virol* 66:1468–1475, 1992.
 31. Hotchkiss RS, Karl IE: The pathophysiology and treatment of sepsis. *N Engl J Med* 348:138–150, 2003.
 32. Russell JA: Management of sepsis. *N Engl J Med* 355:1699–1713, 2006.

